

A PARAMETER-FREE MAP IMAGE RECONSTRUCTION ALGORITHM FOR IMPULSE-BASED UWB GROUND PENETRATING RADAR

Henry C. Ogworonjo, PhD and John M.M. Anderson, PhD

Department of Electrical and Computer Engineering

Howard University, Washington, DC

Lam Nguyen

U.S Army Research Laboratory

Adelphi, Maryland

Overview

- Motivation
- Detection Techniques for Landmines and IEDs
- Introduction to GPR
- Existing Methods for UWB GPR Reconstruction
- Overall Methodology
- GPR Linear Model
- Maximum a Posteriori Estimation
- Majorize-Minimize Optimization Technique
- Parameter-Free Map (PFM) Algorithm
- Conclusions and Acknowledgement

Motivation

- Landmines are self-contained explosive devices that detonate when triggered by a person or vehicle
- Factors that can trigger landmines
 - *Pressure*
 - *Movement*
 - *Sound*
 - *Vibration*
 - *Passage of time*
 - *Signals*
- Types of landmines
 - *Anti-tank*
 - *Anti-personnel*
- Different shapes, casings and materials



Motivation

- Currently more than 50-70 million uncleared landmines in at least 70 countries
- It will take about 1,100 years to remove all landmines at the current clearance rate
- Over 26,000 people are killed or maimed every year by landmines
- Over 1,000,000 casualties reported since 1980 [1]
- Half of all casualties in the Iraq and Afghanistan wars were attributed to land mines and improvised explosive devices (IEDs) [2]



[1] U.S. Department of State, "Hidden Killers: The Global Landmine Crisis", US Department of State Publication

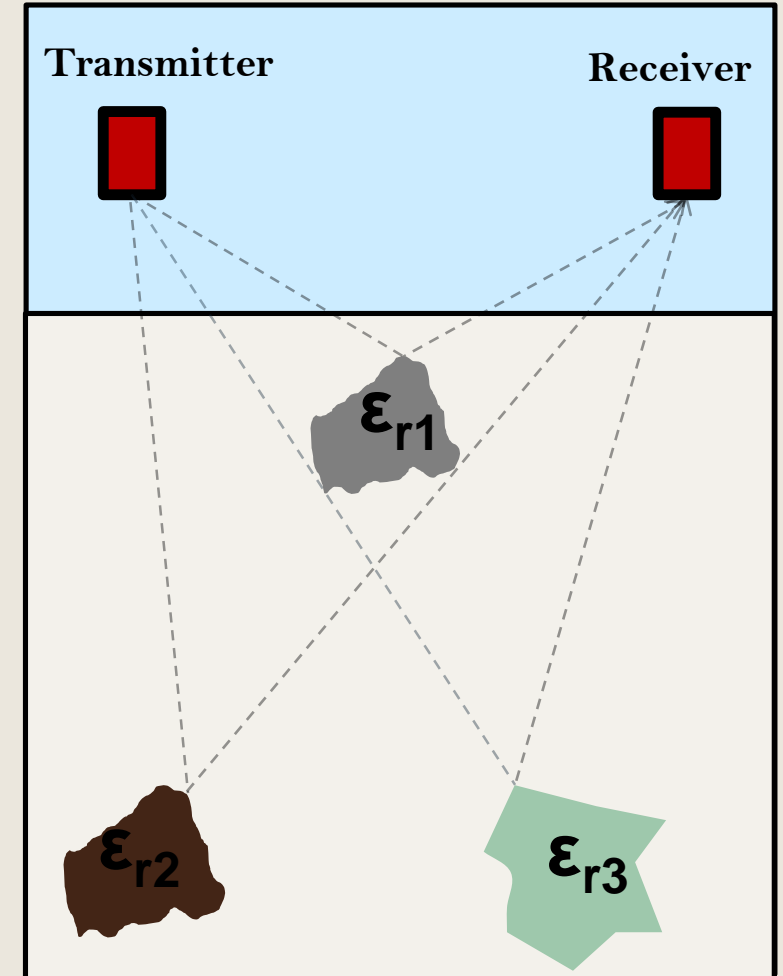
[2] C. Wilson, "Improvised explosive devices (IEDs) in Iraq and Afghanistan: effects and countermeasures". CRS Report for Congress, 2007

Landmines Detection Techniques

- Metal Detector
 - *Based on disturbances from time-varying magnetic field*
 - *Most popular but risky and limited to metallic detection*
- Acoustic/Seismic methods
 - *Based on vibration of materials subjected to sound waves*
 - *Unaffected by moisture and weather but limited by depth of penetration and interference*
- Biological Methods
 - *Use of trained dogs, rats, pigs, birds and bees*
 - *Training required, false alarms common, distraction inevitable*
- Mechanical Methods
 - *Includes prodding and use of mine clearing machines*
 - *Efficient but risky and costly*
- Electromagnetic Methods
 - *Use of microwaves, infrared, X-ray , GPR etc*
 - *Microwaves produce ambiguous results, infrared-based algorithms are not well developed, X-ray results are poor, GPR is promising*

Introduction to GPR

- Electromagnetic pulses are directed at the physical scene-of-interest (SOI)
- Backscatter occurs when the transmitted pulse encounters dielectric constant changes within an SOI
- Backscattered echoes capture the information needed to map the SOI onto the reconstructed imaging space
- Buried targets are expected to have higher dielectric constant values than surrounding material, such as soil and rocks
- GPR data are echoes recorded by receivers for each transmitted pulse



Existing Methods for UWB-GPR Reconstruction

- Delay-and-Sum (DAS)
 - *Fast and straightforward implementation*
 - *Produces images with poor resolution and large side lobes*
- Recursive Sidelobe Minimization (RSM)
 - *Reconstructs images with reduced clutter and has been applied in other SAR applications*
 - *Does not incorporate the a priori information that SOI is sparse*
- Least Absolute Selection and Shrinkage Operator (LASSO)
 - *No straightforward way to choose parameter*
- Sparsity Learning Iterative Method (SLIM)
 - *Involves matrix inversion that may be too computationally intensive for real applications*

Motivation for a Parameter-Free Algorithm



- Determining a suitable choice for the parameter of the prior probability density function is not straightforward
- Cross-validation is an off-line procedure that is time-consuming and sacrifices measurement for validation
- L-curve is an off-line procedure that is computationally expensive for large-size large scale estimation problems

Overall Methodology

- Use the MAP method to incorporate the a priori knowledge that the SOI contains few scatterers
- Use “integrate-out” approach to obtain a hyper-parameter-free prior probability density function
- Solve the resulting MAP objective functions using the majorize-minimize optimization technique
- Jointly estimate noise power

GPR Linear Model

Output of the j^{th} receiver at the i^{th} transmit position

$$s_{ij}(t) = \sum_{l=1}^L x_l \alpha_{ijl} p(t - \tau_{ijl}) + w(t)$$

- x_l : Unknown reflection coefficient at l^{th} terrain pixel
- $p(t)$: Transmitted pulse
- α_{ijl} : Round trip pulse attenuation
- τ_{ijl} : Round trip pulse travel time
- $w(t)$: Noise
- $\{\mathbf{y}_{ij}\}$: sampled GPR data where

$$\mathbf{y}_{ij} = [s_{ij}(0), s_{ij}(T), \dots, s_{ij}((N-1)T)]^T$$

GPR Linear Model (Cont.)

- Model:

$$y = Ax + w$$

- Vector y contains sampled GPR data for I transmit positions and J receivers.
- Vector x contains L unknown reflection coefficients
- System matrix A is $(IJN) \times L$
- Problem Statement: Given y and A , estimate x

Maximum A Posteriori Estimation

- MAP estimate:

$$\hat{x}_{MAP} = \arg \max_x f_{X|Y}(x|y)$$

- Assumptions:

- *Noise is WGN with variance σ^2*
- *Reflection coefficients are independent and identically distributed*

$$\hat{x}_{MAP} = \arg \min_x \frac{1}{2\sigma^2} \|\mathbf{y} - \mathbf{A}\mathbf{x}\|_2^2 + \frac{K}{2} \log \sigma^2 - \log f_{\mathbf{X}}(x)$$

- Prior density function is Laplacian distribution

$$f(a; \lambda) \triangleq \frac{\lambda}{2} \exp(-\lambda|a|)$$

Maximum A Posteriori Estimation (Cont.)

- Integrate-out approach places a noninformative hyperprior over a parameter [3] to give a hyperparameter-free probability density function

$$f_X(\mathbf{x}) = \int_0^{\infty} f_{X|\Lambda}(\mathbf{x}|\lambda) f_{\Lambda}(\lambda) d\lambda$$

- Conditional probability density function is the Laplacian distribution

$$f_{X|\Lambda}(x|\lambda) = \frac{\lambda}{2} e^{-\lambda|x|}$$

- Hyperprior is the Jeffreys' prior for the Laplacian distribution

$$f_{\Lambda}(\lambda) \triangleq [I(\lambda)]^{\frac{1}{2}} \quad (\text{in terms of Fisher's information})$$

$$I(\lambda) = -E_{\lambda} \left[\frac{\partial^2 \log f_{X|\Lambda}(x|\lambda)}{\partial \lambda^2} \right] = \frac{1}{\lambda^2}$$

$$f_{\Lambda}(\lambda) = \frac{1}{\lambda} \quad (\lambda > 0)$$

[3] G.C. Cawley, N.L. Talbot, and M. Girolami, "Sparse multinomial logistic regression via bayesian L1 regularization," *Bioinformatics*, 10, pp. 209-216, 2007.

Maximum A Posteriori Estimation (Cont.)

$$f_X(\mathbf{x}) = \int_0^\infty f_{X|\Lambda}(\mathbf{x}|\lambda) f_\Lambda(\lambda) d\lambda = \int_0^\infty \prod_{l=1}^L \left(\frac{\lambda}{2} \cdot e^{-\lambda|x_l|} \right) \cdot \frac{1}{\lambda} d\lambda$$

- Simplifying and using the gamma integral

$$f_X(\mathbf{x}) = \left[\frac{1}{2^L} \cdot \frac{\Gamma(L)}{(\sum_{l=1}^L |x_l|)^L} \right]$$

- Resulting MAP objective function

$$\phi(x, \sigma^2) = \frac{1}{2\sigma^2} \phi_{LS}(\mathbf{x}) + \frac{K}{2} \log(\sigma^2) + L \cdot \gamma(\mathbf{x})$$

where

$$\phi_{LS}(\mathbf{x}) \triangleq \|\mathbf{y} - \mathbf{Ax}\|_2^2$$
$$\gamma(\mathbf{x}) \triangleq \log \left(\sum_{l=1}^L |x_l| \right)$$

Majorize-Minimize Optimization Technique

- $g(\mathbf{x}, \mathbf{y})$ is a majorizing function of f if
 - a) $g(\mathbf{x}, \mathbf{y}) \geq f(\mathbf{x})$ for all \mathbf{x}, \mathbf{y}
 - b) $g(\mathbf{x}, \mathbf{x}) = f(\mathbf{x})$ for all \mathbf{x}
- MM algorithm
$$\mathbf{x}^{(n+1)} = \arg \min_{\mathbf{x}} g(\mathbf{x}, \mathbf{x}^{(n)})$$
- Property of MM algorithm
$$f(\mathbf{x}^{(n+1)}) \leq f(\mathbf{x}^{(n)})$$
 for all n

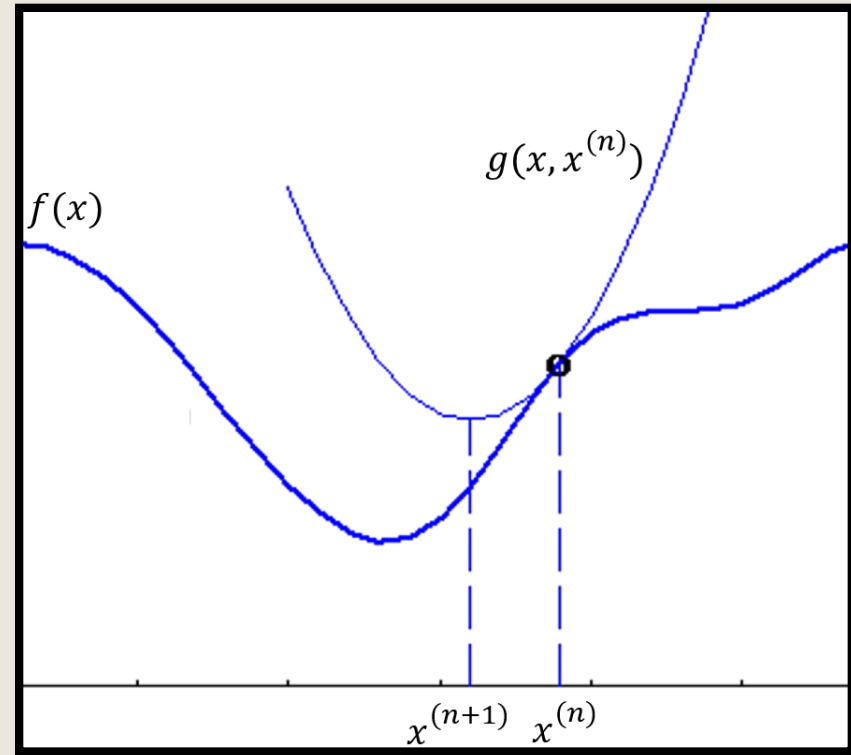


Illustration of MM Concept

PFM Algorithm

Overview:

Suppose Q is a majorizing function for the MAP objective function, ϕ , at the point $\mathbf{x}^{(m)}$. Then,

$$\mathbf{x}^{(m+1)} \triangleq \arg \min_{\mathbf{x}} Q(\mathbf{x}, \sigma^{2(m)}; \mathbf{x}^{(m)})$$

$$\begin{aligned} \sigma^{2(m+1)} &\triangleq \arg \min_{\sigma^2 > 0} \phi(\mathbf{x}^{(m+1)}, \sigma^2) \\ &= \frac{1}{K} \left\| \mathbf{y} - \mathbf{A}\mathbf{x}^{(m+1)} \right\|_2^2 \end{aligned}$$

PFM Algorithm (Cont.)

What is a suitable choice for Q ?

- For any $\mathbf{x} \in \mathbb{R}^n$ and function $h(\mathbf{x})$,

$$\log(h(\mathbf{x})) \leq \log(h(\mathbf{x}^{(m)})) + \frac{h(\mathbf{x})}{h(\mathbf{x}^{(m)})} - 1$$

$$\gamma(x) = \log\left(\sum_{l=1}^L |x_l|\right) \leq \log\left(\sum_{l=1}^L |x_l^{(m)}|\right) + \frac{\sum_{l=1}^L |x_l|}{\sum_{l=1}^L |x_l^{(m)}|} - 1$$

- Using De Leeuw and Lange's [4] majorization function for $|a|$

$$q(\mathbf{x}; \mathbf{x}^{(m)}) = \log\left(\sum_{l=1}^L |x_l^{(m)}|\right) + \frac{\sum_{l=1}^L \frac{\gamma'(x_l^{(m)})}{2x_l^{(m)}} (x_l^2 - x_l^{(m)}) + \gamma(x_l^{(m)})}{\sum_{l=1}^L |x_l^{(m)}|} - 1$$

[4] J. de Leeuw and K. Lange, "Sharp Quadratic Majorization in One Dimension" Computational Statistics and Data Analysis, vol. 53 no.1 pp 2478 February 2004.

PFM Algorithm (Cont.)

- Majorizing function for $\phi_{LS}(\mathbf{x})$

$$\phi_{LS}(\mathbf{x}) = \sum_{k=1}^K y_k^2 - 2 \sum_{k=1}^K y_k [\mathbf{Ax}]_k + \sum_{k=1}^K \left([\mathbf{Ax}^{(m)}]_k \right)^2$$

- De Pierro [5] developed a majorizing function for $\left([\mathbf{Ax}^{(m)}]_k \right)^2$

$$r_k(\mathbf{x}; \mathbf{x}^{(m)}) = \sum_{l=1}^L c_{kl} \left(n_k A_{kl} x_l - n_k A_{kl} x_l^{(m)} + [\mathbf{Ax}^{(m)}]_k \right)^2$$

- Therefore,

$$q_{LS}(\mathbf{x}; \mathbf{x}^{(m)}) = \sum_{k=1}^K y_k^2 - 2 \sum_{k=1}^K y_k [\mathbf{Ax}]_k + \sum_{k=1}^K r_k(\mathbf{x}; \mathbf{x}^{(m)})$$

[5] A.R De Pierro, " A modified expectation Maximization algorithm for penalized likelihood estimation in emission tomography", IEEE transactions, medical imagery, pp 132-137, 1995

PFM Algorithm (Cont.)

Majorizing function for ϕ :

$$\begin{aligned}
 & Q(\mathbf{x}; \mathbf{x}^{(m)}) \\
 &= \frac{1}{2\sigma^2} \sum_{k=1}^K \left(y_k^2 - 2y_k [\mathbf{A}\mathbf{x}]_k + \sum_{l=1}^L c_{kl} \left(n_k A_{kl} x_l - n_k A_{kl} x_l^{(m)} + [\mathbf{A}\mathbf{x}^{(m)}]_k \right)^2 \right) \\
 &+ \frac{k}{2} \log(\sigma^2) + L \cdot \log \left(\sum_{l=1}^L |x_l^{(m)}| \right) + L \cdot \frac{\sum_{l=1}^L \frac{\gamma'(x_l^{(m)})}{2x_l^{(m)}} (x_l^2 - x_l^{(m)}) + \gamma(x_l^{(m)})}{\sum_{l=1}^L |x_l^{(m)}|} - L
 \end{aligned}$$

- Taking the derivative of the majorizing function Q with respect to x_l and setting it to zero yields the desired update for the l^{th} reflectance coefficient

PFM Algorithm (Cont.)

- Updates for reflection coefficients and noise power:

$$x_l^{(m+1)} = \frac{D_l^{(m)} (G_l^{(m)} + x_l^{(m)} H_l)}{D_l^{(m)} + L \cdot \sigma^{2(m)}}, \quad l = 1, 2, \dots, L$$

$$H(l) = \sum_{k=1}^K n_k A_{kl}^2, \quad G^{(m)}(l) = \sum_{k=1}^K A_{kl} (y_k - [Ax^{(m)}]_k)$$

$$D_l^{(m)} = |x_l^{(m)}| \sum_{l=1}^L |x_l^{(m)}|$$

$$\sigma^{2(m+1)} = \frac{1}{K} \|\mathbf{y} - \mathbf{A}x^{(m+1)}\|_2^2$$

PFM Algorithm in Practice

- $\gamma(\mathbf{x})$ is defined as

$$\gamma(\mathbf{x}) \triangleq \log \left(\sum_{l=1}^L |x_l| + c \right)$$

- $c > 0$ insures the parameter-free MAP objective function has a minimizer

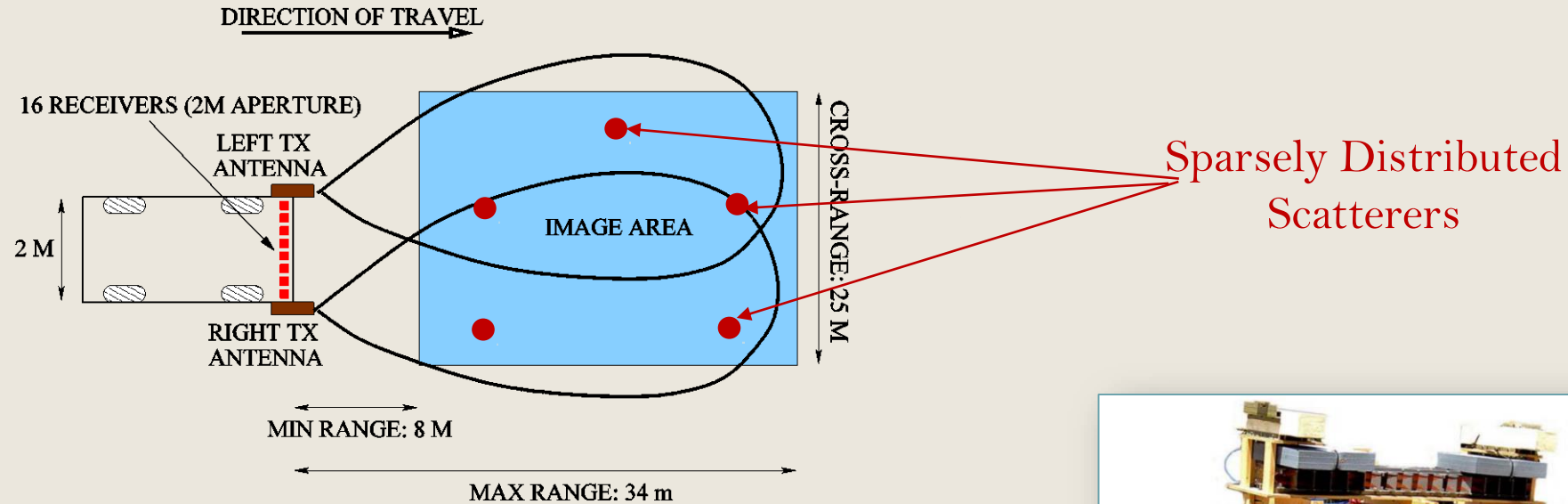
- c is chosen such that

$$\phi(\hat{\mathbf{x}}) < \phi(\mathbf{0})$$

- DAS image is used as initial estimate

- Acceleration techniques for computing $H(l)$ and $G^{(m)}(l)$ from previous work [6] are used for a fast memory-efficient implementation.

Simulation Results: ARL SIRE System



- A monocycle UWB pulse (300 -3000 MHz)
- 2 transmit antennas
- 1 active transmit antenna per shot
- 16 receive antennas



ARL SIRE System
Prototype

Simulation Results: Real Data

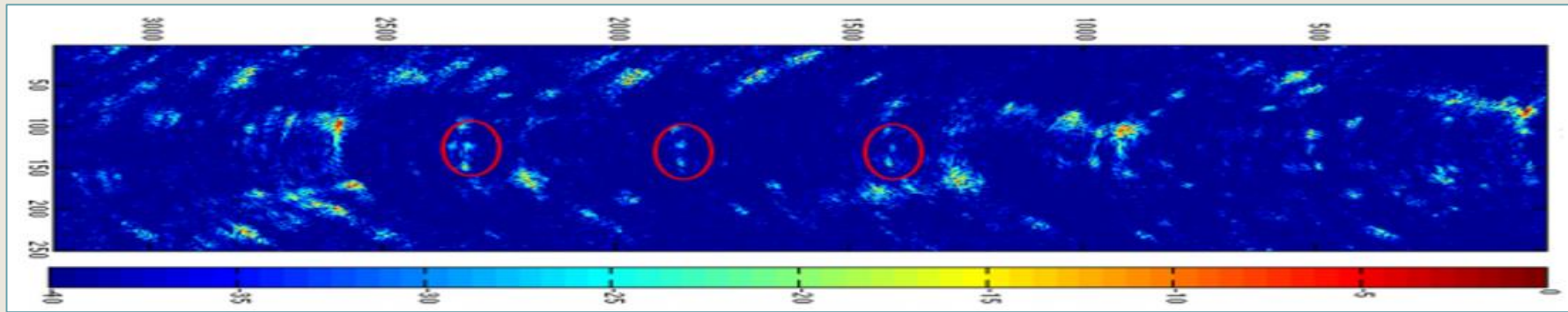


Image formed using DAS algorithm

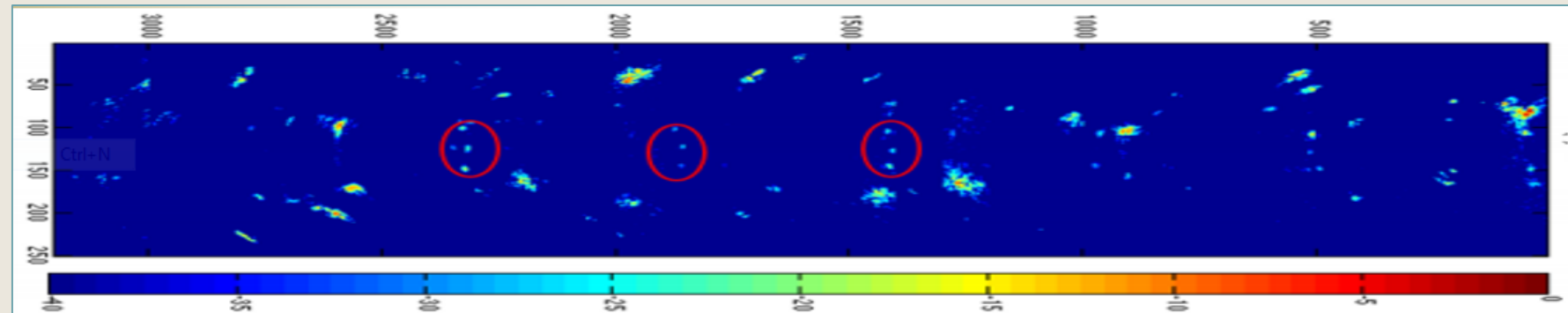


Image formed using LMM algorithm

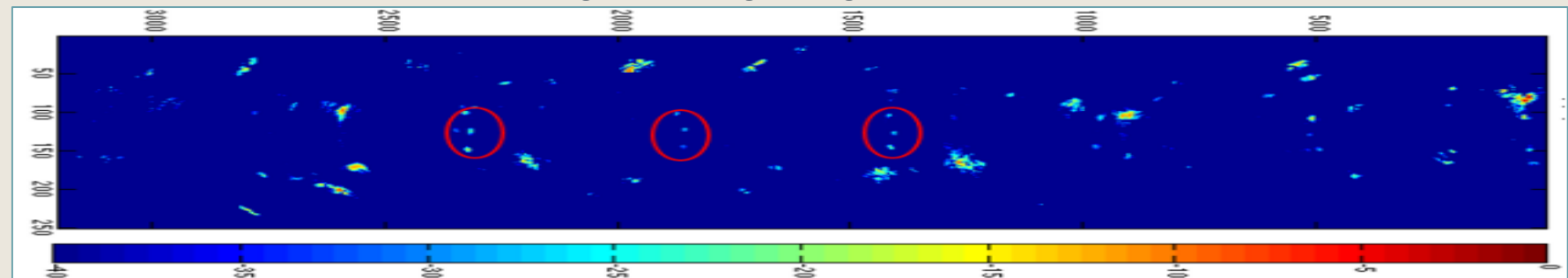
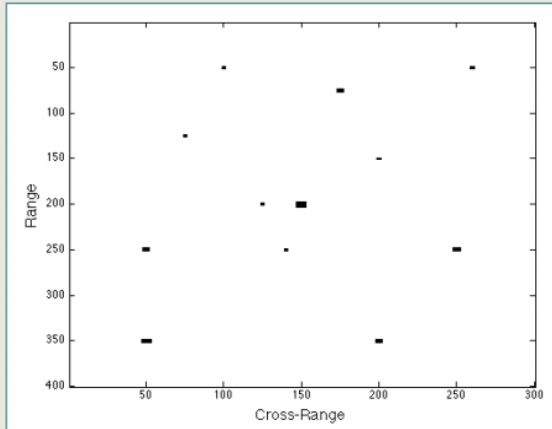
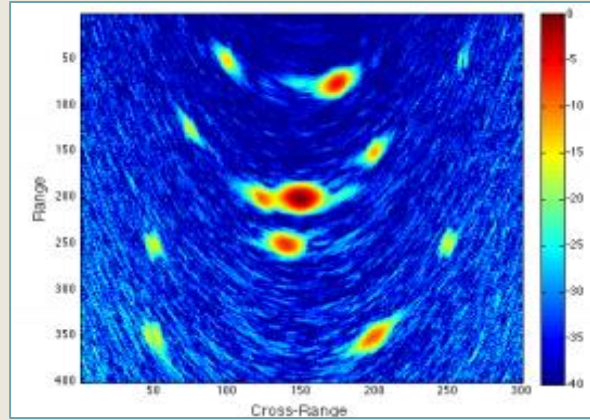


Image formed using PFM algorithm

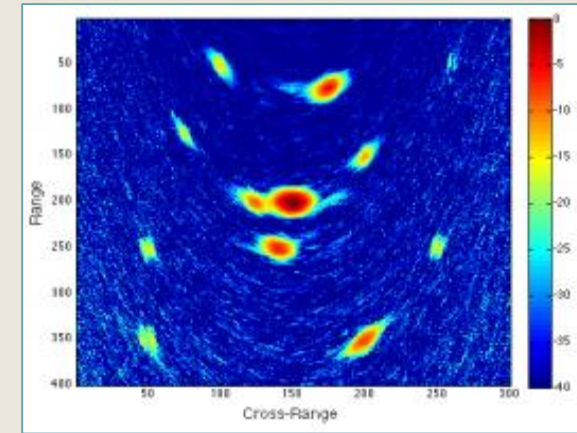
Comparison Using Threshold Detector



True scene-of-interest with 12 point-scatterers



DAS Image for 12 point-scatterers



RSM image for 12 point-scatterers

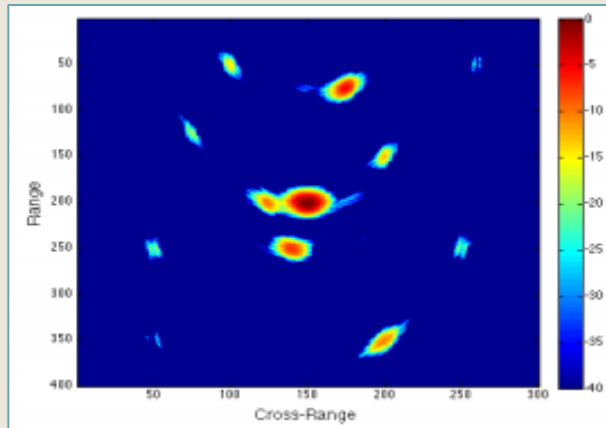
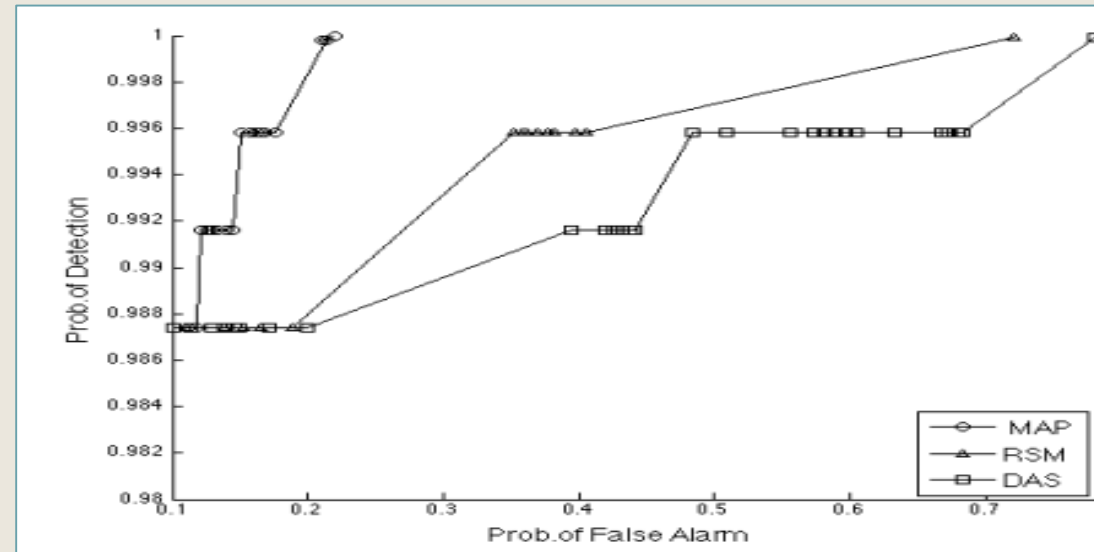


Image formed using PFM algorithm for 12 point-scatterers



ROC comparing DAS, RSM and PFM algorithms for 12 point-scatterers.
SNR=20dB, I= 121, J=16

Conclusions



- Developed Parameter-Free MAP algorithms have been successfully applied to synthetic and real data from the impulse-based ARL SIRE system
- Algorithms produced images that are sparse with suppressed background noise while retaining known scatterers

Acknowledgement

This material is based upon work supported by or in part by, the U.S. Army Research Laboratory and the U.S. Research Office under contract number W911NF-1120039



THANK
YOU!